LIFE PREDICTION OF SATELLITE LITHIUM BATTERY BASED ON MULTI TIME-SCALE EXTENDED KALMAN FILTER (EKF) ALGORITHM

Qian-Qian LIU[1], Bing CHEN[2], Jingyuan ZHANG[3]

State-of-Charge (SOC) and the maximum available capacity estimation are the most important parts of satellite lithium battery life prediction. However, the parameters of the maximum available capacity change slowly compared with the fast time-varying SOC. This paper proposes a multi time-scale of Extended Kalman Filter (EKF) algorithm on SOC and the maximum available capacity for estimation on different time scales. The estimated value of SOC is used as an observation on the macro time-scale to update the maximum available power. The simulation results of experiment on NCA/C space borne lithium battery show that SOC and the maximum available capacity estimation from the proposed multi time-scale EKF algorithm has higher accuracy and computational efficiency compared with Dual EKF.

Keywords: Satellite lithium battery SOC, the maximum available capacity, the venin circuit model, Multi time-scale Extended Kalman Filter (EKF) algorithm

1. Introduction

Lithium batteries are critical to the satellite power distribution systems and are gradually replacing traditional batteries as the third-generation satellites with energy storage [1].Owing to charge, discharge management and performance recession of lithium battery [2], its working state monitoring, performance degradation and residual life prediction (RUL) have become the key in the field of satellite system fault prediction and health management (PHM) research.

The maximum available capacity of battery is often used as degradation characteristics of battery life. Precise SOC estimation can not only be used to assess the reliability of equipment but reflect the residual service life of the battery. In addition to the traditional open circuit voltage method and the ampere-hour integral method, literature [3] [4] [5] analyzed Kalman filter method applied to satellite lithium battery SOC estimation in detail. In Literature [6], the EKF algorithm was improved. The Sigma point set is constructed by using the state quantity and variance matrix. The Kalman filter algorithm based on Sigma point can achieve

[1] College of Electronic Engineering, Naval University of Engineering,WuHan,430033, China; e-mail: liuhe1984@163.com
[2] College of Electronic Engineering, Naval University of Engineering,WuHan,430033, China;
[3] College of Weaponry Engineering, Naval University of Engineering,WuHan,430033, China;

better accuracy. In literature [7], the Kalman filtering algorithm was combined with the ampere-hour method. In literature [8], unscented Kalman filter was used for lithium battery SOC prediction. The dual EKF estimation algorithm put forward in [9] can make real-time SOC and maximum available capacity with voltage and current measurements with noise.

The accuracy of maximum available capacity estimation obtained by using state and parameter estimation technology is poor, which has two reasons. One is that the voltage of the battery is the only measurement, but the connection between the maximum available capacity and the battery voltage is very weak; additionally, due to the strong correlation between SOC and the maximum available capacity, inaccurate maximum available capacity estimation would further lead to inaccurate SOC estimation, and vice versa. In terms of computational efficiency, maximum available capacity is the slow-time variable of indicator system of health (SOH) state [12], [13]. If the maximum available capacity and fast-time variable SOC are operated on the same time scale, which would lead to high computational complexity. In order to solve these difficulties, this paper proposes a multi time-scale EKF algorithm to estimate the SOC and maximum available capacity respectively. Contribution mainly includes: (1) Multi time-scale SOC and the maximum available capacity of time scale separation estimation algorithm are proposed; (2) The estimated SOC is used to update the prediction value of maximum available capacity dynamically. As a technology of ampere-hour method and EKF filtering, this algorithm realized higher precision and efficiency than Dual EKF.

2. Satellite lithium battery system description

2.1Thevenin battery model

The equivalent circuit model of satellite lithium battery is Rint model, RC model; Thevenin model and PNGV model [4] and so on. Thevenin model [9] considered the mutation and gradual change of battery voltage under the excitation of current, the structure is shown in Fig.1.The model parameters described as follows. Uoc is the open circuit voltage (OCV) of battery; R_t is used to describe the charge accumulation and dissipation of battery ohm resistance in double electric layers; R_p describes the battery polarization resistance, C_p describes the battery polarization capacitance. The RC network they constructed is used to simulate the dynamic characteristics of satellite battery showing in the process of generation and elimination in the polarization phenomenon. U_p is the polarization voltage on the RC network, U describes the terminal voltage of battery, I describes the load current of battery (assuming discharge current is positive, and charge current is negative).

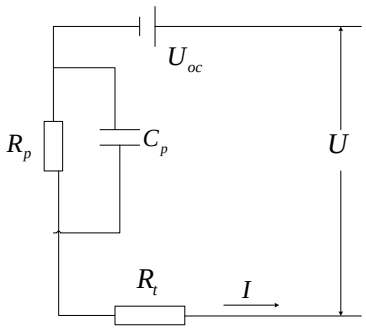

Fig.1 Thevenin equivalent circuit model

SOC is defined as the ratio of available capacity to nominal capacity. When the environment temperature is certain, the relationship between OCV and SOC is not only a reflection of static characteristics of lithium battery [11], but also discernible.

Set $z = SOC$, where $f(z)$ is used to describe the determined relationship between OCV and SOC. It is important to point out that the connection of battery SOC and its terminal voltage has been enhanced through the $f(z)$, which is very important for the improvement of SOC prediction accuracy. It can be known from Fig. 1 that the mathematical relationship of Thevenin model parameters can be expressed as follows:

$$U = U_{oc} - U_p - IR_t = f(z) - U_p - IR_t \tag{1}$$

$$\dot{U}_p = -U_p / (R_p C_p) + I / C_p \tag{2}$$

Ampere-hour method is the simplest SOC estimation method which is currently used more frequently [14], [15]. It makes integral calculation with the current flowing through the battery in run-time to calculate the flowing in or out of battery. If the initial battery SOC value is available, it can be used for obtaining the battery remaining power. Eq. (3) is the foundation of SOC state equation:

$$SOC = 1 - (\int i \cdot \eta \cdot dt) / Q \tag{3}$$

where i is the current, Q is the maximum available power consumption, t is the time and η is Coulomb effective factor, which is defined as the ratio required by charging and discharging energy restoring to the original power. η is less than or equal to 1. For example, in the discharge model, when the minimum discharge voltage is reached, it is thought that the battery has been completely discharged, and SOC is 0.

Through the combination of Thevenin equivalent circuit model and Ampere-hour method, the battery parameters, SOC and its terminal voltage are associated. Taking SOC, polarization voltage U_p as state variables, state Eq. is obtained as follows:

$$\begin{cases} SOC = 1 - (\int i \cdot \eta \cdot dt) / Q \\ \dot{U}_p = -U_p / (R_p C_p) + I / C_p \end{cases} \tag{4}$$

Taking terminal voltage U as measurement value, the observation Eq. is:

$$U = f(z) - U_p - IR_t \tag{5}$$

2.2 Discretization model of multi time-scale

The application object of EKF is nonlinear discrete systems, therefore, the continuous model in the above section needs discretization. For systems with very different parameter variations, we can set two-time scales: the macroscopic time-scale and the microscopic time-scale. The system volume on the macro time-scale changes slowly with time but on the micro time-scale, it changes rapidly with time.

For convenience, k and l is used as time index of macro time-scale and micro time-scale. Any moment can be expressed as $t_{k,l}$, and there are relationships: $t_{k,l} = t_{k,0} + l \cdot T$, $t_{k,0} = t_{k-1,L}$ ($l = 1,2,...,\mathrm{L}$, $k = 1,2,...,\infty$), T is a fixed time interval between two adjacent points. It should be noticed that L represents the level of time-scale separation. According to the change of system parameters, simulation time steps k of the macro time-scale can be determined; between time step k and k+1 , according to the change of system state variable, the sampling period T can also be determined, i.e. the micro simulation time steps l is determined. Considering that the model parameters is slow time-varying ,we assume that the battery is the time-invariant system, and load current is constant at each sampling interval T .Then we can get the analytic solution Eq. (2):

$$U_p((l+1)T) = \exp(-\frac{T}{R_p C_p}) U_p(lT) + \int_0^T \exp(-\frac{t}{R_p C_p}) dt \cdot \frac{I(lT)}{C_p} \tag{6}$$

Battery model shown in Fig. 1 takes State of Charge z and polarization voltage U_p as state variables, load current I as the input, terminal voltage U as output, it obtains after discretization in multi time-scale:

$$U_{k,l}^p = \exp(-\frac{T}{R_p C_p}) \cdot U_{k,l-1}^p + (1 - \exp(-\frac{T}{R_p C_p})) \cdot R_p I_{k,l} \tag{7}$$

Set $z_{k,l} = SOC$, Eq. (8) is obtained from Eq. (3),

$$z_{k,l} = z_{k,l-1} - \frac{\eta I_{k,l-1} T}{Q} \tag{8}$$

Set $\tau_p = R_p \cdot C_p$, Eq. (9) is obtained from Eq. (4) to (8),

$$\begin{bmatrix} U_{k,l}^{p} \\ z_{k,l} \end{bmatrix} = \begin{bmatrix} \exp(-\frac{T}{\tau}) & 0 \\ 0 & 1 \end{bmatrix} \begin{bmatrix} U_{k,l-1}^{p} \\ z_{k,l-1} \end{bmatrix} + \begin{bmatrix} (1-\exp(-\frac{T}{\tau}))R \\ -\eta T / Q \end{bmatrix} I_{k,l} \tag{9}$$

The discretization state transition and measurement Eq. on multi time-scale are,

$$\begin{cases} x_{k,l+1} = \begin{bmatrix} \exp(-\frac{T}{\tau}) & 0 \\ 0 & 1 \end{bmatrix} x_{k,l} + \begin{bmatrix} (1-\exp(-\frac{T}{\tau}))R_t \\ -\eta T / Q \end{bmatrix} u_{k,l} \\ y_{k,l} = f(z_{k,l}) - U_{k,l}^{p} - R_t u_{k,l} \end{cases} \tag{10}$$

where $x_{k,l} = [z_{k,l} \quad U_{k,l}^{p}]^T$, $\theta_k = Q_k$, $u_{k,l} = I_{k,l}$, $y_{k,l} = U_{k,l}$, and $U_{k,l}$ is the measurement value of the battery terminal voltage at $t_{k,l}$.

In order to make the following discussion be more general, Eq. (10) is changed to the following nonlinear state space model,

$$\begin{aligned} &\text{Transition：} x_{k,l+1} = F(x_{k,l}, u_{k,l}, \theta_k) + w_{k,l}, \quad \theta_{k+1} = \theta_k + r_k \\ &\text{Measurement：} y_{k,l} = G(x_{k,l}, u_{k,l}, \theta_k) + v_{k,l} \end{aligned} \tag{11}$$

where, $x_{k,l}$ is the system state vector at time $t_{k,l} = t_{k,0} + l \cdot T$, $l = 1,2,...,L$, T is the fixed time interval between the neighboring measurement point. It should be noticed that L represents the level of time separation, and $x_{k,0} = x_{k-1,L}$. θ_k is the vector of system model parameters at $t_{k,0}$; $u_{k,l}$ is the input of external observation source; $y_{k,l}$ is the vector of system observation value or measurement value. $w_{k,l}$ and r_k are process noise vector of state and model parameters. $v_{k,l}$ is the vector of measurement voice, $F(x_{k,l}, u_{k,l}, \theta_k)$ and $G(x_{k,l}, u_{k,l}, \theta_k)$ are the functions of state transition and state measurement, respectively.

3. Multi time-scale EKF algorithm

As for the discrete model of the system on the multi time-scale, multi time-scale EKF algorithm is used to predict the SOC and maximum available capacity. Multi time-scale EKF algorithm prediction process is divided into six steps, macro EKF and micro EKF execute together in the form of a nested loop. Within each macro time step k, macro EKF executes time update step, state prediction step and measurement update step. Within each micro time step l, micro EKF executes time update step and measurement update step. When $l = 1$ cycles to $l = L$, the macro time step k ends and enters into the next macro time step k+1. Regardless of macro or micro EKF, they both needs to get the experience value based on prior information to model parameters θ and state x for initialization before conduction. Covariance matrix $\sum_{\theta}$ and $\sum_{x}$ for estimation error make initialization according

to priori information too. Basic steps are summarized in Table 1.

Table 1.

Multi time-scale EKF algorithm steps

Steps	Contents	
Step 1	initialization $\hat{\theta}_0=E[\hat{\theta}_0],\ \sum_{\theta_{k,l}}=E[(\theta_0-\hat{\theta}_0)(\theta_0-\hat{\theta}_0)^T]$ $\hat{x}_{0,0}=E[x_{0,0}],\ \sum_{x_{k,l}}=E[(x_{0,0}-\hat{x}_{0,0})(x_{0,0}-\hat{x}_{0,0})^T]$ On macro-scale $k\in\{1,...,\infty\}$,	(12)
Step 2	time update of macro EKF $\hat{\theta}_k^- = \hat{\theta}_{k-1},\quad \sum_{\theta_k}^- = \sum_{\theta_{k-1}} + \sum_{r_{k-1}}$	(13)
Step 3	State prediction of macro EKF $\tilde{x}_{k-1,L} = F_{0\to L}(\hat{x}_{k-1,0}, u_{k-1,L-1}, \hat{\theta}_k^-)$	(14)
Step 4	Measurement update of macro EKF	
	$K_k^\theta = \sum_{\theta_k}^- (C_k^\theta)^T [C_k^\theta \sum_{\theta_k}^- (C_k^\theta)^T + \sum_{n_k}]^{-1}$	(15)
	$\hat{\theta}_k = \hat{\theta}_k^- + K_k^\theta[\hat{x}_{k-1,L} - \tilde{x}_{k-1,L}],\ \sum_{\theta_k} = (1-K_k^\theta C_k^\theta)\sum_{\theta_k}^-$	(16)
	On micro-scale $l\in\{1,...,L\}$,	
Step 5	Time update of micro EKF	
	$\hat{x}_{k,l}^- = F(\hat{x}_{k,l-1}^-, u_{k,l-1}, \hat{\theta}_{k-1}),\ \sum_{x_{k,l}}^- = A_{k,l-1}\sum_{x_{k,l-1}} A_{k,l-1}^T + \sum_{w_{k,l-1}}$	(17)
Step 6	Measurement update of micro EKF	
	$K_{k,l}^x = \sum_{x_{k,l}}^- (C_{k,l}^x)^T [C_{k,l}^x \sum_{x_{k,l}}^- (C_{k,l}^x)^T + \sum_{v_{k,l}}]^{-1}$	(18)
	$\hat{x}_{k,l} = \hat{x}_{k,l}^- + K_{k,l}^x[y_{k,l} - G(\hat{x}_{k,l}^-, u_{k,l}, \hat{\theta}_{k-1})],\quad \sum_{x_{k,l}} = (I - K_{k,l}^x C_{k,l}^x)\sum_{x_{k,l}}^-$	(19)
	Where, $A_{K,l-1} = \left.\frac{\partial F(x, u_{k,l-1}, \hat{\theta}_{k-1})}{\partial x}\right\|_{x=\hat{x}_{k,l-1}}, C_{k,l}^x = \left.\frac{\partial G(x, u_{k,l}, \hat{\theta}_{k-1})}{\partial x}\right\|_{x=\hat{x}_{k,l}^-}$	(20)
	$C_k^\theta = \left.\frac{dF_{0\to L}(\hat{x}_{k-1,0}, u_{k-1,0:L-1}, \theta)}{d\theta}\right\|_{\theta=\hat{\theta}_k^-}$	(21)

3.1. Macro EKF

Within each macro time step, parameter estimation value $\hat{\theta}_k^-$ and $\sum_{\theta_k}^-$ at the previous step are calculated according to Eq. (13). And then we use micro EKF for predictive state according to Eq. (14), $F_{0\to L}(x_{k-1,0}, u_{k\text{-}1,L\text{-}1}, \theta_k^-)$ is the iteration form of state transfer function $F(x_{k,l}, u_{k,l}, \theta_k)$ in Eq. (11). Compare with the time and measurement update, the computational complexity needed by $F_{0\to L}(x_{k-1,0}, u_{k\text{-}1,L\text{-}1}, \theta_k^-)$ calculation on micro time step L. On the measurement update procedures, predicted state calculated by macro EKF and micro EKF estimation state value are different, and difference is used to obtain the posteriori

parameter estimation, seen Eq. (16). Macro EKF has two distinct features: since it update S on the macro scale $(L \cdot T)$, the computational complexity is greatly reduced; macro EKF makes state estimation from micro EKF firstly and then updates the measurement. According to the Eq. (14) for state prediction achievement, the parameter estimated value generated is decoupling through state prediction.

3.2 EKF Micro EKF

As for state transition, micro EKF uses the estimated value of maximum available capacity achieved in the above macro time step procedure (seen Eq. (17)). It is worth mentioning that in the initiation of each macro time steps, i.e., $t_{k-1,0}$, micro EKF sends a state estimation value to macro EKF, and then predicts the state according to the state of Eq. (14) at the macro time step. After completing the state prediction at each macro step, i.e., $t_{k-1,L-1}$, micro EKF sends another state estimated value to macro EKF to compare with the predicted estimation and use its difference for correcting the parameter estimation value in the measurement update procedure of Eq. (16).

3.3 Numerical implementation: Recursive differential calculation

On the Multi time-scale EKF algorithm, C_k^{θ} calculation in macro EKF involves in the total derivative of the state prediction function concerning the parameters:

$$C_k^{\theta} = \left. \frac{dF_{0\to L}(\hat{x}_{k-1,0}, u_{k-1,0}, \theta)}{d\theta} \right|_{\theta=\hat{\theta}_k^-} \tag{22}$$

State amount x is also the function concerning system parameter θ, therefore, the total derivative is needed to split into partial derivative for circulated calculation. The following Eq. can be obtained:

$$\frac{dF_{0\to L}(\hat{x}_{k-1,0}, u_{k-1,0}, \theta)}{d\theta} = \frac{\partial F_{0\to L}(\hat{x}_{k-1,0}, u_{k-1,0:L-1}, \theta)}{\partial \theta} + \frac{\partial F_{0\to L}(\hat{x}_{k-1,0}, u_{k-1,0:\ L-1}, \theta)}{\partial \hat{x}_{k-1,0}} \frac{d\hat{x}_{k-1,0}}{d\theta} \tag{23}$$

$$\frac{d\hat{x}_{k\text{-}1,0}}{d\theta} = \frac{d\hat{x}_{k\text{-}1,0}^-}{d\theta} - K_{k,l-1}^x \frac{dG_{0\to L}(\hat{x}_{k\text{-}1,0}^-, u_{k\text{-}1,0:\ L-1}, \theta)}{d\theta} \tag{24}$$

$$\frac{dG_{0\to L}(\hat{x}_{k,0}^-, u_{k,0:\ L-1}, \theta)}{d\theta} = \frac{\partial G_{0\to L}(\hat{x}_{k,0}^-, u_{k,0:\ L-1}, \theta)}{\partial \theta} + \frac{\partial G_{0\to L}(\hat{x}_{k,0}^-, u_{k,0:\ L-1}, \theta)}{\partial \hat{x}_{k,0}^-} \frac{d\hat{x}_{k,0}^-}{d\theta} \tag{25}$$

$$\frac{d\hat{x}_{k,0}^-}{d\theta} = \frac{\partial F_{0\to L}(\hat{x}_{k-1,0}^-, u_{k-1,0:\ L-1}, \theta)}{\partial \theta} + \frac{\partial G_{0\to L}(\hat{x}_{k-1,0}^-, u_{k-1,0:\ L-1}, \theta)}{\partial \hat{x}_{k-1,0}^-} \frac{d\hat{x}_{k-1,0}}{d\theta} \tag{26}$$

C_k^{θ} can be obtained according to the recursive calculation of Eq.s (23)-(26). The partial derivative of state prediction parameters on state x and parameter θ can be calculated easily according to the confirmed function form.

3.4 Multi time-scale EKF algorithm to predict the satellite lithium battery SOC calculation process

Next, the EKF prediction algorithm execution process of satellite lithium battery system with multi time-scale is introduced in this paper. Flow chart is shown in Fig. 2. Algorithm consists of two parallel extended Kalman filters; the upper part (micro EKF) modifies SOC on the micro time-scale, the lower part (macro EKF) modifies the power availability estimation value on macro time scale. Micro EKF sends SOC estimation value to macro EKF and receives maximum available capacity estimation value from macro EKF.

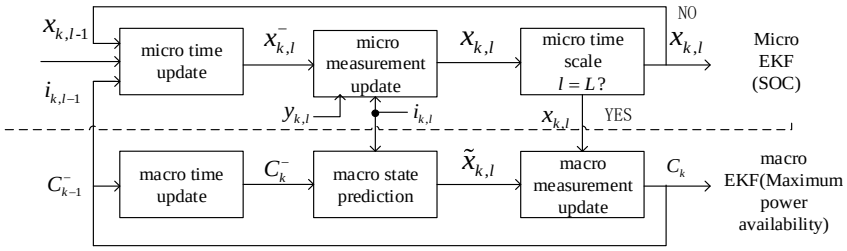

Fig.2 Multi time-scale estimation flow chart of satellite lithium battery SOC based on EKF

4. Simulation and Experiment Result

4.1 Experimental process

The NCA/C spaceborne lithium battery we used in this experiment is 1.6Ah. Test system includes comprehensive test equipment of satellite lithium battery, the temperature sensor module, NCA/C spaceborne lithium batteries, and the special install fixture. Test equipment can support 8 channels for experiment at the same time. According to the local test results, we use the data of battery No.37 for identification and simulation. The NCA/C spaceborne lithium battery used in the experiment and the experiment equipment are shown in Fig. 3.

4.1.1 Relationship identification of open circuit voltage Uoc - SOC

The process of model parameter identification and satellite lithium battery SOC estimation are both involved in the relationship identification between EMF (Electromotive Force) and SOC. Because EMF cannot be obtained by circuit experiment directly, the present researches mostly use the balanced voltage when battery opens, which is OCV to replace EMF; OCV and EMF are thought equal approximately. In section 2.1, the battery open circuit voltage (OCV) is replaced with $f(z)$, identified results are shown in Fig. 4.

(a) NCA/C spaceborne lithium battery (b) comprehensive test equipment of satellite lithium battery

Fig.3 satellite lithium battery and experiment equipment.

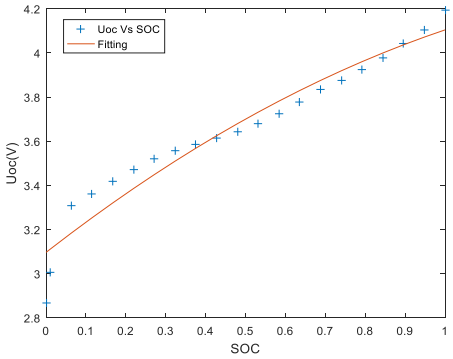

Fig.4 Open voltage and SOC relationship Fitting

It can be seen from Fig.4 that with the rising of SOC, open circuit voltage is almost a linear relationship at 0.3<SOC<0.9; the open circuit voltage changes dramatically when SOC < 0.2. Therefore, the relationship fitting between open circuit voltage at 0.3<SOC<0.9 and SOC is:

$$Uoc = -0.39909 \cdot SOC^2 + 1.4069 \cdot SOC + 3.0966 \tag{27}$$

4.1.2 Model parameter identification

Thevenin equivalent circuit model contains parameter R_t, R_p and C_p, which are needed to be identified before using the model. Experiments are conducted under 25 $^{\circ}C$ and the results of each parameter identification as shown in Fig.5:
We found that in the process of discharge, although the change ranges of R_p and C_p is larger, but the change trend is relatively stable. It can be seen that the change trends of them are on the contrary, which makes $\tau_p = R_p C_p$ change little; R_t fluctuates in the range of 0.032 Ω to 0.033 Ω, and there is no certain linear rule.

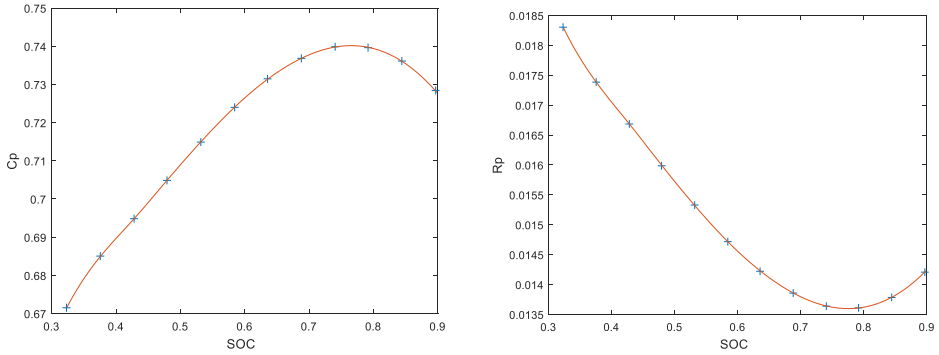

(a) is the relationship curve of discharge direction R_p and SOC;

(b) is the relationship curve of discharge direction C_p and SOC;

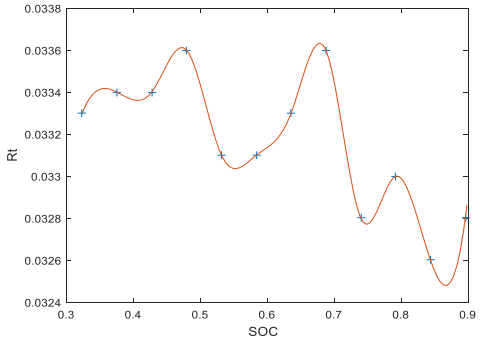

(c) is the relationship curve of discharge direction R_t and SOC.

Fig. 5 The relationship between the parameters (The red line is the fitted curve; discrete points represent the true value of identification experiment).

4.1.3 Experimental verification under the custom working condition

After model parameter identification complementation, the prediction model of satellite lithium battery SOC and maximum available capacity on multi time-scale is established. The discharge experiment under a set of custom working condition is used to test the estimation performance of the algorithm put forward on SOC. The custom condition test scheme used is as follows: firstly, let the battery fully rest, then discharges 500 seconds with the constant current 0.5 C=0.8A, rest 50 seconds. And then let battery charge 50 seconds with the constant current 0.5 C=0.8A. Repeat the above steps, 12 times in all. The experiment current is shown in Fig. 6. The experimental current is loaded to test equipment of satellite lithium battery according to the custom working condition. The current and voltage data of the battery is extracted after the experiment. The battery parameters obtained in the previous experiment corresponded to SOC from 0.3 to 0.9, in order to match the parameters, SOC in this experiment all changes from 0.3 to 0.9. This section uses Dual EKF and multi time-scale EKF algorithm respectively in the MATLAB

software for offline verification on NCA/C lithium battery SOC and maximum available capacity estimation. Experiment is carried out fewer than 25 $^{\circ}C$.

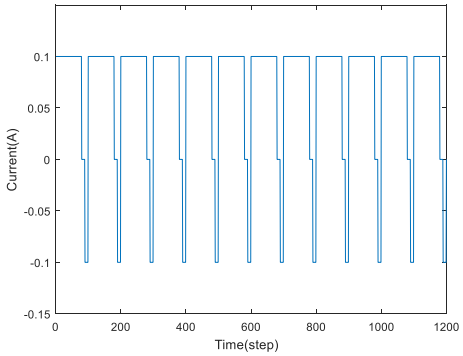

Fig. 6 Experiment current of the custom working condition

4.2 Experimental results and analysis

Thevenin equivalent circuit model is established in the MATLAB software, the input signal for simulation experiment is current of the custom working condition. SOC obtained using Dual EKF [11] and the curve of maximum available capacity estimation is shown in Fig. 7.

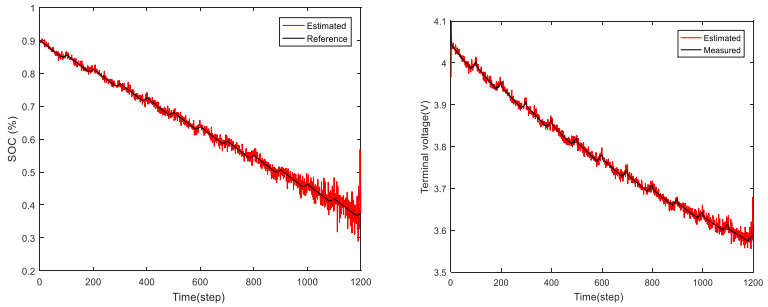

(a) is the relationship of terminal voltage prediction value and measurement value;
(b) is the relationship of SOC estimation value and truth-value;

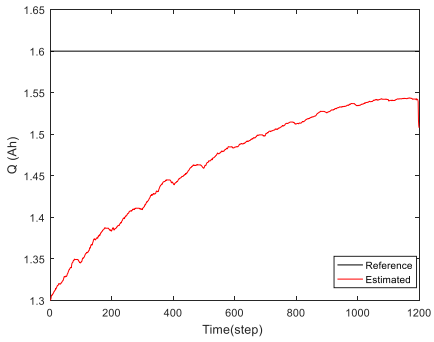

(c) is the relationship of system parameter Q estimation value and truth-value.
Fig.7 Simulation results of Dual EKF.

The curve of NCA/C spaceborne lithium battery SOC and maximum available capacity prediction obtained using multi time-scale EKF algorithm is shown Fig. 8.

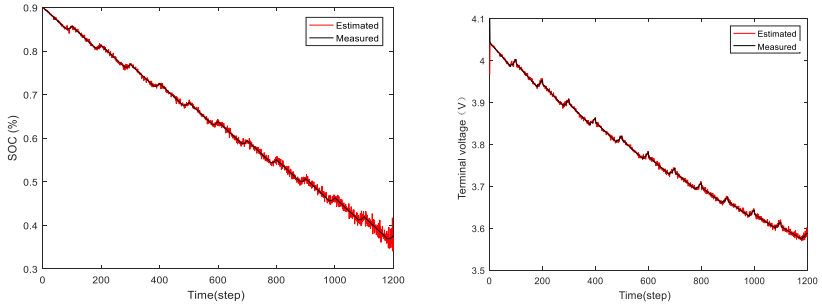

(a) is the relationship of terminal voltage prediction value and measurement value;

(b) is the relationship of SOC estimation value and truth-value;

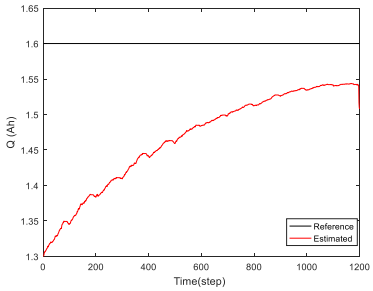

(c) is the relationship of system parameter Q estimation value and truth-value.

Fig.8 Estimation results of multi time-scale EKF algorithm.

In terms of maximum available capacity estimation, the initial values we set are both less than the true values in the two methods, as shown in Fig. 7 (c) and Fig. 8(c). From Fig. 7 (c), it can be known that estimation of the maximum available capacity failed to closely track the real maximum available capacity; eventually, the estimated value converged in about 4.3% error range and includes larger noise. In Fig. 8(c), the estimated value is converged to the true maximum available capacity gradually as the simulation steps increases. The accuracy of Dual EKF is low due to measurement in SOC and maximum available capacity estimation and time scale coupling. As shown in Eq. (28), for modifying the prediction value of maximum available capacity, Dual EKF uses terminal voltage of the battery as the measurement value to modify it.

$$\hat{\theta}_{k,l}^{-} = \hat{\theta}_{k,l}^{-} + K_{k,l}^{\theta}(\mathrm{y}_{k,l} - G(\hat{x}_{k,l}^{-}, u_{k,l})) \tag{28}$$

The difference is that multi time-scale EKF algorithm makes estimation on maximum available capacity according to Eq. (29) and (30) on the macro scale. It avoids the terminal voltage of the battery is the only measurement for the parallel estimation process of SOC and the maximum available capacity.

$$\tilde{x}_{k-1,L} = F_{0\to L}(\hat{x}_{k-1,0}, u_{k-1,L-1}, \hat{\theta}_k^-) \tag{29}$$

$$\hat{\theta}_k = \hat{\theta}_k^- + K_k^{\theta}[\hat{x}_{k-1,L} - \tilde{x}_{k-1,L}] \tag{30}$$

Moreover, there is no direct relationship between the observations Eq. $G(\hat{x}_{k,l}^-, u_{k,l})$ and the maximum available capacity. When we use observed quantity to update the maximum available capacity, it just relies on the measurement of White Gaussian Noise on the Kalman filter processing, with limited effect. Meanwhile, the state variable $x_{k,l} = [z_{k,l} \quad U_{k,l}^p]^T$ and the maximum available capacity have a direct connection. Using the state variable for parameters updating can produce more reliable maximum available capacity estimation value.

Compare Fig. 7(a) and Fig. 8 (a), it is easy to see that simulation values of the terminal voltage with multi time-scale are more closely following the measured value change and contains less noise. The error of SOC estimation value in Fig. 8 (a) is smaller than Fig. 7 (a). The dependency of SOC estimation on the maximum available capacity is larger; the deficiency of the maximum available capacity estimation accuracy would reduce the veracity of SOC estimation. Multi time-scale EKF algorithm provides a more accurate maximum available capacity estimation value and SOC estimation is more accurate. Multi time-scale EKF algorithm improves the prediction performance than Dual EKF to a certain extent.

In addition, the two methods are also compared in computational efficiency, shown in table 2. In order to minimize the influence of randomness, the two methods are carried out 10 times, and then take average for comparison. The time of the average calculation is summarized in Table 2.

Table 2.

Computational efficiency contrast

Algorithm Type	computing time	efficiency Improvement
Dual EKF [11]	0.552	——
Multi time-scale EKF algorithm	0.522	5.43%

It can be observed that multi time-scale EKF algorithm consumes less computation time than Dual EKF. This helps to reduce the burden of computation and the hardware in satellite fault prediction and health management (PHM) system, also improve the PHM system application flexibility and efficiency.

5. Conclusion

The multi time-scale EKF algorithm is an effective and accurate state and parameter estimation method for engineering systems with time-scale separation. In this paper, the multi time-scale EKF algorithm is used to predict the SOC of the satellite lithium battery on the microscopic scale, and the SOC estimation is used as the observation to forecast the maximum available electricity. The effect is better

than the dual EKF estimation, and the calculation is improved effectiveness. The next step will be to establish a satellite lithium battery equivalent model and OCV and SOC relationship model, taking into account the impact of temperature on the SOC, the impact of electricity on the OCV, etc., to improve the accuracy of the model to obtain more accurate estimates.

REFERENCES

[1] *Yuping Wu, Churong Wan, Changying Jiang,* Secondary Battery of Lithium Ion, Chemical Industry Press, 20012:1-10.

[2] *Goebel, Kai, et al.* "Prognostics in battery health management." *IEEE instrumentation &measurement magazine* 11.4 (2008): 33-40.

[3] *Plett, Gregory L.* "Extended Kalman filtering for battery management systems of LiPB-based HEV battery packs: Part 1. Background." *Journal of Power Sources* 161.2(2006):262-276.

[4] *Plett, Gregory L.* "Extended Kalman filtering for battery management systems of LiPB-based HEV battery packs: Part 2. Modeling and identification." *Journal of power sources* 134.2 (2004): 262-276.

[5] *Arman Amini Badr, Navid Taghizadegan Kalantari.* " Reliability evaluation of radial distribution systems including distributed generation based on an improved classification algorithm", U.P.B. Sci. Bull., Series C, Vol. 79, Iss. 4, 2017.pp:211-228

[6] *Plett, Gregory L.* "Sigma-point Kalman filtering for battery management systems of LiPB-based HEV battery packs: Part 1: Introduction and state estimation." Journal of Power Sources 161.2 (2006): 1356-1368.

[7] *Huaizhong Chen,* Application of improved Particle Swarm Optimization algorithm in Maximum Power Point Tracking for PV system. U.P.B. Sci. Bull., Series C, Vol. 79, Iss. 4, 2017.pp:179-192

[8] *He, Wei, et al.* "State of charge estimation for Li-ion batteries using neural network modeling and unscented Kalman filter-based error cancellation." *International Journal of Electrical Power & Energy Systems* 62 (2014): 783-791.

[9] *Lee, Seongjun, et al.* "State-of-charge and capacity estimation of lithium-ion battery using a new open-circuit voltage versus state-of-charge." *Journal of power sources* 185.2 (2008): 1367-1373.

[10] *Rahimi-Eichi, H., F. Baronti, and M-Y. Chow.* "Modeling and online parameter identification of Li-Polymer battery cells for SOC estimation." *Industrial Electronics (ISIE), 2012 IEEE International Symposium on*. IEEE, 2012.

[11] *Simon D. Optimal state estimation: Kalman, H-infinity, and nonlinear approaches.* John Wiley & Sons, 2006.

[12] *Goebel, Kai, et al.* "Prognostics in battery health management." IEEE instrumentation & measurement magazine 11.4 (2008): 33-40.

[13] *Santhanagopalan S, Zhang Q, Kumaresan K, et al.* Parameter estimation and life modeling of lithium-ion cells. Journal of the Electrochemical Society, 2008, 155(4): A345-A353.

[14] *Mi C, Li B, Buck D, et al.* Advanced electro-thermal modeling of lithium-ion battery system for hybrid electric vehicle applications. IEEE Vehicle Power and Propulsion Conference. IEEE, 2007: 107-111.

[15] *Fuller T F, Doyle M,* Newman J. Simulation and optimization of the dual lithium ion insertion cell. Journal of the Electrochemical Society, 1994, 141(1): 1-10.